

Equation of state of cold and dense QCD matter in resummed perturbation theory

Yuki Fujimoto and Kenji Fukushima

*Department of Physics, The University of Tokyo,
7-3-1 Hongo, Bunkyo-ku, Tokyo 113-0033, Japan*

We discuss the Hard Dense Loop resummation at finite quark mass and evaluate the equation of state (EoS) of cold and dense QCD matter in β equilibrium. The resummation in the quark sector has an effect of lowering the baryon number density and the EoS turns out to have much smaller uncertainty than the perturbative QCD estimate. Our numerical results favor smooth matching between the EoS from the resummed QCD calculation at high density and the extrapolated EoS from the nuclear matter density region. We also point out that the speed of sound in our EoS slightly exceeds the conformal limit.

Introduction: A reliable estimate of the equation of state (EoS) of cold matter at high baryon density is a vital challenge in theoretical nuclear physics. In various circumstances such as the neutron star cores, the neutron star mergers emitting gravitational waves, the supernova explosion, and the heavy-ion collisions to scan over the phase diagram of matter made out of quarks and gluons (see Ref. [1] for a review on the present status and the future direction of the heavy-ion collision), the EoS is an indispensable input for theoretical studies. Conversely, experimental data available from these extreme environments provide us with useful constraints on possible EoSs, so that some theoretical scenarios can be excluded/accepted. The most well-known and successful example along these lines is the establishment of two-solar-mass neutron stars [2], which disfavors scenarios leading to soft EoS; namely, it is unlikely for dense matter to accommodate a strong first-order phase transition [3] nor condensations of exotic degrees of freedom.

The most advanced first-principles approach from the fundamental theory of the strong interaction, i.e., quantum chromodynamics (QCD) is the lattice Monte-Carlo simulation, but the notorious sign problem ruins the importance sampling algorithm for matter at finite baryon density. Still, in parameter space where the lattice-QCD simulation is at work, the validity of alternative theoretical approaches has been tested. In particular, the Hard Thermal Loop perturbation theory (HTLpt) is the most promising resummation scheme [4–8] that confronts the lattice-QCD results at high temperature T . The purpose of this Letter is to quantify the resummation effects on the EoS of cold and dense quark matter at high baryon density n_B or the energy density ε .

To sharpen novelties in our work, let us briefly summarize what has been understood so far. Since the seminal works of Refs. [9, 10], we had to wait for about three decades until the perturbative QCD (pQCD) EoS was augmented with the strange quark mass $M_s \neq 0$ and applied to the neutron star phenomenology [11, 12], where they found that the strange mass effect is crucial. The obstacle in utilizing the pQCD EoS in neutron star physics was found to be poor convergence in the intermediate

density region (i.e., denser than the nuclear terrain but not dense enough to justify pQCD) and the theoretical efforts are progressing toward further higher-order calculations [13] with hope for better convergence.

From the success of HTLpt at high T , it is a natural anticipation that the same machinery of resummation would cure the convergence problem at high baryon density or large quark chemical potential μ as well. Indeed, the parallelism between the high T and high μ cases has been established based on the transport equation approach in Ref. [14]; the high-density counterparts of HTLs are called Hard Dense Loops (HDLs). As long as a resummation prescription in the quark sector is concerned, more simply, we can just take the $T \rightarrow 0$ limit of HTLpt to introduce “HDLpt” as considered in Ref. [15] (see also Ref. [5], and we note that the term “HDLpt” was first introduced in Ref. [16]). The HTL approximation usually neglects the bare quark mass and only the screening masses of quarks enter expressions used in Refs. [5, 15]. Later on, extensive discussions about the EoS and the quark star properties have been addressed in Ref. [16]. As seen in Fig. 2 of Ref. [16], however, the HDLpt hardly remedies the convergence problem associated with uncertainty of the scale $\bar{\Lambda} = \mu - 4\mu$ in the running coupling constant $\alpha_s(\bar{\Lambda})$. In the present work, as in Ref. [12], we will employ the two-loop formula; $\alpha_s(\bar{\Lambda}) = [1 - 2(\beta_1/\beta_0^2) \ln^2(\bar{\Lambda}^2/\Lambda_{\overline{\text{MS}}}^2)/\ln(\bar{\Lambda}^2/\Lambda_{\overline{\text{MS}}}^2)] 4\pi/[\beta_0 \ln(\bar{\Lambda}^2/\Lambda_{\overline{\text{MS}}}^2)]$, where $\beta_0 \equiv (11N_c - 2N_f)/3$, $\beta_1 \equiv (17/3)N_c^2 - N_f(N_c^2 - 1)/(2N_c) - (5/3)N_fN_c$, and we will take $\Lambda_{\overline{\text{MS}}} = 378$ MeV throughout, following Ref. [12]. Previously, the absence of the bare quark mass significantly simplified technicalities as well as the realization of the β equilibrium. With equal amount of u , d , and s quarks (that is automatically the case if their masses are all neglected), the electric charge neutrality follows as it is. For quantitative descriptions of the neutron star phenomenology, however, we need to take account of the strange quark mass and solve the β equilibrium condition.

There seems to be a long way left, but the phenomenological analyses are in need of the QCD-based EoS usable for the neutron star observables. In fact, on top of

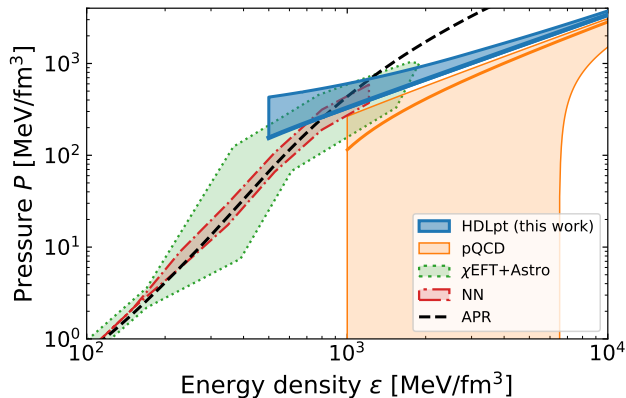


FIG. 1. Comparison of the EoS in this work (HDLpt) and other EoSs. The blue and the orange bands represent our results and the preceding results from Refs. [12, 23], respectively, with $\bar{\Lambda} = \mu - 4\mu$. The green band is from the χ EFT [24]. The red band shows the EoS inferred from the Neural Networks in the machine learning analysis of the neutron star observation [22]. The dashed black line is the APR EoS extrapolated from the nuclear side [25].

extrapolated EoSs from the nuclear side, the Bayesian analysis has been recognized as a powerful instrument for the inference analysis to identify the most likely EoS based on the observational data [17–19] (see Ref. [20] for a review). Recently, the Machine Learning technique has been also advocated as a complementary method to infer the EoS [21, 22]. It would be of utmost importance to make a direct comparison of the inferred EoS candidates and the QCD-based estimates. To this end, we are urged to reduce uncertainty and widen the validity region of the pQCD or HDLpt calculations.

In this Letter we will report the first successful attempt to construct a better convergent EoS from the HDLpt framework incorporating the strange quark mass effect. From the technical point of view, we adopt the resummation schemes in the gluon sector as prescribed in Ref. [4] and in the quark sector as in Ref. [15] with our own extension to cope with the strange quark mass. Our expressions are given in the form of exact integrations without any expansion in terms of the screening mass as in Ref. [7].

Central results: Since technical details are cumbersome, we shall first present our central results in Fig. 1 and then proceed to technical details later. Not to make the comparison on the figure too busy, we chose only a few representative EoSs from the nuclear side; namely, the EoS extrapolated from the chiral Effective Field Theory (χ EFT) calculation [24] by the green band, the Neural Network output in the machine learning analysis [22] by the red band, and the Akmal-Pandharipande-Ravenhall (APR) EoS [25] shown by the dashed line.

The orange band in the region, $\varepsilon > 10^3$ MeV/fm³, rep-

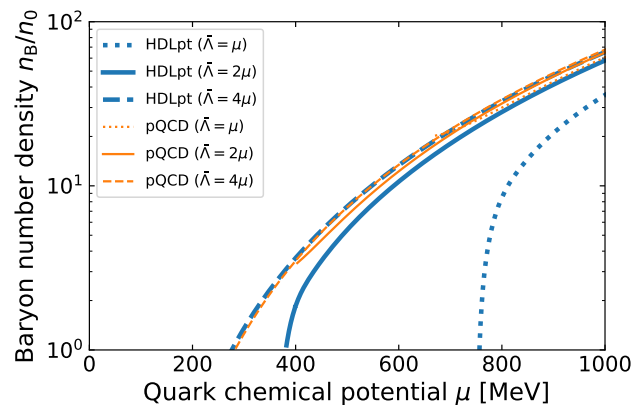


FIG. 2. Baryon number density as a function of the quark chemical potential. In the figure pQCD refers to the results from Refs. [12, 23] and HDLpt to our results.

resents the results from pQCD [12] for which we utilize the concise formula as given in Ref. [23]. Higher-order corrections could be added, but the uncertainty band is not much changed from Ref. [12]. The uncertainty band width abruptly diverges, from which it has been said that pQCD is reliable only at extreme high densities far from reality. At a glance, indeed, we should understand how difficult it is to make a robust interpolation between the nuclear and the pQCD EoSs. Now, a surprise comes from a blue narrow band that represents results from our HDLpt calculations. The uncertainty band is drastically reduced and the HDLpt EoS appears to be merged into the nuclear EoSs smoothly in the intermediate density region. It should be noted that the APR EoS overshoots ours, but this is due to a well-known flaw in the APR EoS, i.e., superluminal speed of sound which violates causality.

One may wonder what causes such a drastic difference on Fig. 1. We can qualitatively understand this from Fig. 2 in which the baryon number density n_B as a function of the quark chemical potential μ is plotted. Because the HDLpt sums the quark loops up, n_B is the most sensitive quantity affected by the resummation in the quark sector. It is an interesting and reasonable observation that n_B is suppressed at fixed μ after the resummation: thermodynamic quantities are dominated by quark quasi-particles, and in HDLpt, quark excitations are more screened by self-energy insertions, as compared to pQCD treatments. Therefore, on Fig. 1, the corresponding μ for a given ε becomes larger, and the corresponding running coupling $\alpha_s(\bar{\Lambda} = \xi\mu)$, where $\xi = 1, 2, 4$, is smaller. This qualitative argument partially accounts for the reduction of the uncertainty band, but not fully yet. If we plot the pressure P and the energy density ε as functions of μ , respectively, the uncertainty bands are not such narrow as in Fig. 1. Nevertheless, $P(\varepsilon)$ with $\bar{\Lambda} = \mu$ and that with $\bar{\Lambda} = 4\mu$ happen to stay close, which

narrows the uncertainty band on Fig. 1. There might be a deep reason (e.g., scaling properties) for this behavior, and further investigations are in progress.

Formulation: Let us explain the formulae and procedures to obtain our results in Fig. 1. Dense matter in the neutron star reaches the β equilibrium; $d \rightleftharpoons u + e^- + \bar{\nu}_e$ and $s \rightleftharpoons u + e^- + \bar{\nu}_e$ indicating the relations between quark chemical potentials as $\mu_u = \mu + \frac{2}{3}\mu_Q$ and $\mu_d = \mu_s = \mu - \frac{1}{3}\mu_Q$ where μ_Q is the electric chemical potential. Since electrons are negatively charged, $\mu_e = -\mu_Q$, and we can fix μ_Q from the charge neutrality, i.e., $n_Q - n_e = 0$ with $n_Q = \partial P/\partial\mu_Q$ and $n_e = \mu_e^3/(3\pi^2)$ neglecting the electron mass.

Since the most crucial extension in this work is the inclusion of the bare quark mass, we will write down the explicit expressions in the quark sector. In our notation for flavor- f quarks the bare mass is M_f and the screening mass is m_{qf} . The bare mass should be scale dependent as

$$M_f(\bar{\Lambda}) = M_f(2\text{GeV}) \left[\frac{\alpha_s(\bar{\Lambda})}{\alpha_s(2\text{GeV})} \right]^{\gamma_0/\beta_0} \frac{1 + \mathcal{A}(\bar{\Lambda})}{1 + \mathcal{A}(2\text{GeV})}. \quad (1)$$

Here, β_0 was already introduced when $\alpha_s(\bar{\Lambda})$ appeared before, and $\gamma_0 \equiv 3(N_c^2 - 1)/(2N_c)$. The two-loop corrections appear in $\mathcal{A}(\bar{\Lambda}) \equiv A_1(\alpha_s(\bar{\Lambda})/\pi) + \frac{A_1^2 + A_2}{2}(\alpha_s(\bar{\Lambda})/\pi)^2$ with $A_1 \equiv -\beta_1\gamma_0/(2\beta^2) + \gamma_1/(4\beta_0)$ and $A_2 \equiv \gamma_0/(4\beta_0^2)(\beta_1^2/\beta_0 - \beta_2) - \beta_1\gamma_1/(8\beta_0^2) + \gamma_2/(16\beta_0)$. For β_2 , γ_1 , and γ_2 , the general expressions are complicated, and we refer to numerical values, $\beta_2 = 3863/24$, $\gamma_1 = 182/3$, and $\gamma_2 = 8885/9 - 160\zeta(3) \approx 794.9$ for $N_c = N_f = 3$. Readers can consult Eq. (8) of Ref. [12] for the complete expressions.

In the $T \rightarrow 0$ limit the HDLpt pressure, P_{HDLpt} , is given by the gluon loop and the quark loop with the self-energy insertions; namely,

$$P_{\text{HDLpt}} = (N_c^2 - 1)P_g + N_c \sum_{f=u,d,s} P_{q,f} + \Delta P_{g,q}, \quad (2)$$

where ΔP_g and ΔP_q subtract the ultraviolet divergences. The gluon part with an appropriate subtraction by $\Delta P_g \propto 1/\epsilon$ (where the spatial dimensions are $d = 3 - 2\epsilon$ in the dimensional regularization) is

$$P_g = \frac{m_D^4}{64\pi^2} \left(\ln \frac{\bar{\Lambda}}{m_D} + C_g \right). \quad (3)$$

A constant, C_g , is an integral over a function involving the gluon self-energy and numerically estimated as $C_g \approx 1.17201$ in the dimensional regularization. Here, m_D is the gluon screening mass induced by μ , i.e., $m_D^2 \equiv (2\alpha_s/\pi) \sum_f \mu_f^2$. We note that the bare quark masses in the hard loops are neglected commonly in the HTL approximation (see Ref. [26] for a standard textbook). The gluon sector is intact, so we just refer to Refs. [4, 6, 7] for further details.

The quark part appears from the flavor- f quark loop, i.e., $P_{q,f} = \text{tr} \ln G_f^{-1}$ where $G_f^{-1} = \not{k} - M_f - \Sigma(k_0, \mathbf{k})$ and $k_0 = i\tilde{\omega}_n + \mu_f$ for flavor- f quarks with $\tilde{\omega}_n$ being the fermionic Matsubara frequency. For the self-energy expression, Σ , we need to introduce the following notations according to Refs. [7, 15], i.e., $A_0(k_0, k) \equiv k_0 - (m_{qf}^2/k_0)\tilde{\mathcal{T}}(k_0, k)$, $A_s(k_0, k) \equiv k + (m_{qf}^2/k)[1 - \tilde{\mathcal{T}}(k_0, k)]$, and the flavor- f quark screening mass is $m_{qf}^2 \equiv (\alpha_s/2\pi)(N_c^2 - 1)/(2N_c)\mu_f^2$. The fermionic HTLpt function in $d = 3 - 2\epsilon$ spatial dimensions is:

$$\tilde{\mathcal{T}}(k_0, k) = {}_2F_1\left(\frac{1}{2}, 1; \frac{3}{2} - \epsilon; \frac{k^2}{k_0^2}\right). \quad (4)$$

Then, the self-energy for flavor- f quarks is expressed as $\not{k} - \Sigma(k_0, k) = A_0(k_0, k)\gamma^0 - A_s(k_0, k)\boldsymbol{\gamma} \cdot \hat{\mathbf{k}}$.

The paramount advance in this work is the inclusion of bare mass M_f , and the quark pressure deviates from Refs. [7, 15]. Let us first write down our final expression and then explain the notations next. In the flavor- f quark sector the pressure contribution reads:

$$P_{q,f} = m_{qf}^4 \left[C_q(\eta_f) + D_q(\eta_f) \ln \frac{\bar{\Lambda}}{m_{qf}} \right] + P_{\text{qp},f} + P_{\text{Ld},f}. \quad (5)$$

We introduced C_q and D_q as functions of $\eta_f \equiv 1 + M_f^2/(2m_{qf}^2)$. These definitions involve the following functions:

$$f_{\pm}(\bar{\omega}, \eta_f) = \frac{\eta_f \pm \eta'(\bar{\omega}, \eta_f)}{1 + \bar{\omega}^2}, \quad (6)$$

$$\eta'(\bar{\omega}, \eta_f) = \sqrt{\eta_f^2 - (1 + \bar{\omega}^2)} \left[(1 - \tilde{\mathcal{T}}(i\bar{\omega}, 1))^2 + \frac{\tilde{\mathcal{T}}^2(i\bar{\omega}, 1)}{\bar{\omega}^2} \right], \quad (7)$$

where $\bar{\omega}$ is a dimensionless and continuous variable. Then, C_q and D_q are given by

$$C_q(\eta_f) = \sum_{\chi=\pm} \frac{1}{4\pi^3} \int_0^\infty d\bar{\omega} \left(f_\chi^2 \ln f_\chi - \frac{\partial f_\chi^2}{\partial \epsilon} \right) + \left(\frac{5}{4} - \ln 2 \right) D_q(\eta_f), \quad (8)$$

$$D_q(\eta_f) = - \sum_{\chi=\pm} \frac{1}{2\pi^3} \int_0^\infty d\bar{\omega} f_\chi^2. \quad (9)$$

We note that $D_q(\eta_f \rightarrow 1) \rightarrow 0$ and $C_q(\eta_f \rightarrow 1) \approx -0.03653$ as is consistent with Ref. [7].

The next term, $P_{\text{qp},f}$, in Eq. (5) is the quasi-particle contribution given by

$$P_{\text{qp},f} = \frac{1}{\pi^2} \int_0^\infty dk k^2 \sum_{\chi=\pm 1} [(\mu_f - \omega_{f\chi})\theta(\mu_f - \omega_{f\chi})] - \frac{\mu_f^4}{12\pi^2}. \quad (10)$$

We note that the ideal term $\propto \mu_f^4$ is subtracted in the above expression since we doubly pick up two pole

contributions at $\omega_{f\pm}$. In Ref. [15] the quasi-particle contribution was defined by taking the m_{qf}^2 derivative/integration, so that only the difference from the ideal term was considered by construction, and the ideal term was not subtracted but added. Here, the quasi-particle poles, $\omega_{f\pm}$, are solutions of the following implicit equations, i.e.,

$$0 = \omega_{f\pm} - \frac{m_{qf}^2}{k} Q_0\left(\frac{\omega_{f\pm}}{k}\right) \mp \sqrt{M_f^2 + \left[k - \frac{m_{qf}^2}{k} Q_1\left(\frac{\omega_{f\pm}}{k}\right)\right]^2} \quad (11)$$

with $Q_0(x) \equiv (1/2) \ln[(x+1)/(x-1)]$ and $Q_1(x) \equiv xQ_0(x) - 1$ being the Legendre functions. Finally, the last term in Eq. (5) represents the contribution from the Landau damping, which reads:

$$P_{\text{Ld},f} = -\frac{1}{\pi^3} \int_0^{\mu_f} d\omega \int_{\omega}^{\infty} dk k^2 \theta_{qf}(\omega, k; M_f, m_{qf}^2). \quad (12)$$

The integrand is given by $\tan \theta_{qf} = \mathcal{Y}/\mathcal{X}$ where

$$\mathcal{X} = k^2 - \omega^2 + M_f^2 + 2m_{qf}^2 + \frac{m_{qf}^4}{k^2} \left\{ 1 - \frac{2\omega}{k} Q_0(k/\omega) - \frac{k^2 - \omega^2}{k^2} \left[Q_0^2(k/\omega) - \frac{\pi^2}{4} \right] \right\}, \quad (13)$$

$$\mathcal{Y} = \frac{\pi m_{qf}^4}{k^2} \left[\frac{\omega}{k} + \frac{k^2 - \omega^2}{k^2} Q_0(k/\omega) \right]. \quad (14)$$

In this case $k \geq \omega$ holds and the argument of Q_0 should be k/ω , not ω/k . We also note that the subtraction at finite M_f is mass dependent, i.e., $\Delta P_q = m_{qf}^4 D_q(\eta_f)/(2\epsilon)$.

For numerical calculations, we took $M_u = M_d = 0$ and $M_s(2\text{GeV}) = 100\text{ MeV}$. For N_c and N_f in $\alpha(\bar{\Lambda})$ and $M_s(\bar{\Lambda})$ we took $N_c = N_f = 3$. This completes the explanation of the formulation necessary to draw Fig. 1.

Discussions: The EoS from our resummed perturbation theory has a notable feature in addition to the improved convergence. We have calculated the speed of sound, $c_s^2 = \partial P/\partial \varepsilon$, which is depicted in Fig. 3. To make clear the relevance to the neutron star environment, we chose the horizontal axis as the baryon number density n_B in the unit of the normal nuclear density n_0 .

There is an empirical conjecture to claim that the speed of sound may not exceed the conformal limit, i.e., $c_s^2 = 1/3$. In the high density limit, asymptotically, all mass scales and interactions are negligible and the conformal limit should be eventually saturated. In the pQCD calculation, the first correction from the conformal limit is negative, so that the conformal limit is approached from $c_s^2 < 1/3$ with increasing density. Also at finite temperature, the lattice-QCD results demonstrate that the conformal bound $c_s^2 < 1/3$ holds [27]. Known examples of QCD calculations seem to respect the conformal limit

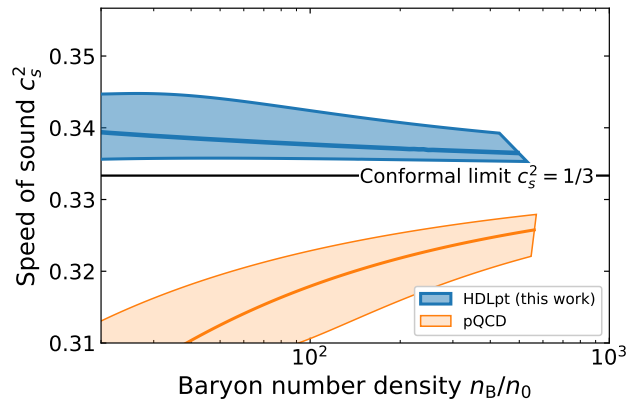


FIG. 3. Speed of sound c_s^2 from the EoSs; the blue band represent the results from our HDLpt EoS, and the orange band from the pQCD for reference.

(see Ref. [28] for an exception at finite isospin chemical potential). However, no field-theoretical proof exists to guarantee $c_s^2 < 1/3$. The recent analysis based on neutron star data, especially the two-solar-mass condition, indeed suggest a possibility of $c_s^2 > 1/3$ at sufficiently high baryon density [29–31].

Figure 3 shows that our resummed EoS slightly violates the conformal bound and c_s^2 approaches $1/3$ from above. It is evident that our result is a counterexample to the conjecture of $c_s^2 < 1/3$. The quantitative difference is numerically small between EoSs from our HDLpt and pQCD, and the violation of the conformal bound is tiny, but this comparison on Fig. 3 implies that one should be careful about the robustness of the speed of sound bound (see, for example, discussions in Refs. [32]).

Summary: In this Letter we showed results with the better convergence for the cold dense matter EoS in the form of $P(\varepsilon)$. The formalism we adopted here is the HDLpt, which has already been successful in finite temperature QCD. The important observation is that, as compared to the pQCD calculation, quarks are screened by self-energy insertions, and the baryon density is suppressed. This means that the corresponding chemical potential for a given baryon density is shifted to be larger, which amends the convergence problem. We also emphasize the importance of the inclusion of a bare quark mass and we numerically solved the β equilibrium and charge neutrality conditions. Our treatments with the bare quark mass are messy, but contributions from finite strange quark mass are crucial for the realistic environments of neutron stars under the β equilibrium. Our results constitute a QCD-based example of the conformal limit violation at finite density, which can be in consonance with the state-of-the-art neutron star observations. It would be an exciting program to apply our EoS to the neutron star phenomenology. We will report phenomeno-

logical implications soon.

The authors thank Yuya Abe for useful discussions. This work was supported by Japan Society for the Promotion of Science (JSPS) KAKENHI Grant Nos. 18H01211, 19K21874 (KF) and JP20J10506 (YF).

-
- [1] K. Fukushima, B. Mohanty, and N. Xu, (2020), [arXiv:2009.03006 \[hep-ph\]](#).
- [2] P. Demorest, T. Pennucci, S. Ransom, M. Roberts, and J. Hessels, *Nature* **467**, 1081 (2010), [arXiv:1010.5788 \[astro-ph.HE\]](#); E. Fonseca *et al.*, *Astrophys. J.* **832**, 167 (2016), [arXiv:1603.00545 \[astro-ph.HE\]](#); J. Antoniadis *et al.*, *Science* **340**, 6131 (2013), [arXiv:1304.6875 \[astro-ph.HE\]](#); H. Cromartie *et al.* (NANOGrav), *Nature Astron.* **4**, 72 (2019), [arXiv:1904.06759 \[astro-ph.HE\]](#).
- [3] M. G. Alford, G. Burgio, S. Han, G. Taranto, and D. Zappalà, *Phys. Rev. D* **92**, 083002 (2015), [arXiv:1501.07902 \[nucl-th\]](#).
- [4] J. O. Andersen, E. Braaten, and M. Strickland, *Phys. Rev. Lett.* **83**, 2139 (1999), [arXiv:hep-ph/9902327 \[hep-ph\]](#); *Phys. Rev.* **D61**, 014017 (2000), [arXiv:hep-ph/9905337 \[hep-ph\]](#).
- [5] J. O. Andersen, E. Braaten, and M. Strickland, *Phys. Rev. D* **61**, 074016 (2000), [arXiv:hep-ph/9908323](#).
- [6] N. Haque, A. Bandyopadhyay, J. O. Andersen, M. G. Mustafa, M. Strickland, and N. Su, *JHEP* **05**, 027 (2014), [arXiv:1402.6907 \[hep-ph\]](#).
- [7] S. Mogliacci, J. O. Andersen, M. Strickland, N. Su, and A. Vuorinen, *JHEP* **12**, 055 (2013), [arXiv:1307.8098 \[hep-ph\]](#).
- [8] J. Ghiglieri, A. Kurkela, M. Strickland, and A. Vuorinen, (2020), [arXiv:2002.10188 \[hep-ph\]](#).
- [9] B. A. Freedman and L. D. McLerran, *Phys. Rev. D* **16**, 1130 (1977); *Phys. Rev. D* **16**, 1147 (1977); *Phys. Rev. D* **16**, 1169 (1977).
- [10] V. Baluni, *Phys. Rev. D* **17**, 2092 (1978).
- [11] E. S. Fraga and P. Romatschke, *Phys. Rev.* **D71**, 105014 (2005), [arXiv:hep-ph/0412298 \[hep-ph\]](#).
- [12] A. Kurkela, P. Romatschke, and A. Vuorinen, *Phys. Rev.* **D81**, 105021 (2010), [arXiv:0912.1856 \[hep-ph\]](#).
- [13] T. Gorda, A. Kurkela, P. Romatschke, M. Säppi, and A. Vuorinen, *Phys. Rev. Lett.* **121**, 202701 (2018), [arXiv:1807.04120 \[hep-ph\]](#).
- [14] C. Manuel, *Phys. Rev. D* **53**, 5866 (1996), [arXiv:hep-ph/9512365](#).
- [15] R. Baier and K. Redlich, *Phys. Rev. Lett.* **84**, 2100 (2000), [arXiv:hep-ph/9908372 \[hep-ph\]](#).
- [16] J. O. Andersen and M. Strickland, *Phys. Rev.* **D66**, 105001 (2002), [arXiv:hep-ph/0206196 \[hep-ph\]](#).
- [17] F. Özel, G. Baym, and T. Guver, *Phys. Rev. D* **82**, 101301 (2010), [arXiv:1002.3153 \[astro-ph.HE\]](#).
- [18] A. W. Steiner, J. M. Lattimer, and E. F. Brown, *Astrophys. J.* **722**, 33 (2010), [arXiv:1005.0811 \[astro-ph.HE\]](#).
- [19] D. Alvarez-Castillo, A. Ayriyan, S. Benic, D. Blaschke, H. Grigorian, and S. Typel, *Eur. Phys. J. A* **52**, 69 (2016), [arXiv:1603.03457 \[nucl-th\]](#).
- [20] F. Özel and P. Freire, *Ann. Rev. Astron. Astrophys.* **54**, 401 (2016), [arXiv:1603.02698 \[astro-ph.HE\]](#).
- [21] Y. Fujimoto, K. Fukushima, and K. Murase, *Phys. Rev. D* **98**, 023019 (2018), [arXiv:1711.06748 \[nucl-th\]](#).
- [22] Y. Fujimoto, K. Fukushima, and K. Murase, *Phys. Rev. D* **101**, 054016 (2020), [arXiv:1903.03400 \[nucl-th\]](#).
- [23] E. S. Fraga, A. Kurkela, and A. Vuorinen, *Astrophys. J. Lett.* **781**, L25 (2014), [arXiv:1311.5154 \[nucl-th\]](#).
- [24] K. Hebeler, J. M. Lattimer, C. J. Pethick, and A. Schwenk, *Phys. Rev. Lett.* **105**, 161102 (2010), [arXiv:1007.1746 \[nucl-th\]](#).
- [25] A. Akmal, V. R. Pandharipande, and D. G. Ravenhall, *Phys. Rev.* **C58**, 1804 (1998), [arXiv:nucl-th/9804027 \[nucl-th\]](#).
- [26] M. Le Bellac, *Thermal Field Theory*, Cambridge Monographs on Mathematical Physics (Cambridge University Press, 1996).
- [27] S. Borsanyi, Z. Fodor, C. Hoelbling, S. D. Katz, S. Krieg, and K. K. Szabo, *Phys. Lett. B* **730**, 99 (2014), [arXiv:1309.5258 \[hep-lat\]](#); A. Bazavov *et al.* (HotQCD), *Phys. Rev. D* **90**, 094503 (2014), [arXiv:1407.6387 \[hep-lat\]](#).
- [28] D. T. Son and M. A. Stephanov, *Phys. Rev. Lett.* **86**, 592 (2001), [arXiv:hep-ph/0005225 \[hep-ph\]](#).
- [29] P. Bedaque and A. W. Steiner, *Phys. Rev. Lett.* **114**, 031103 (2015), [arXiv:1408.5116 \[nucl-th\]](#).
- [30] I. Tews, J. Carlson, S. Gandolfi, and S. Reddy, *Astrophys. J.* **860**, 149 (2018), [arXiv:1801.01923 \[nucl-th\]](#).
- [31] C. Drischler, S. Han, J. M. Lattimer, M. Prakash, S. Reddy, and T. Zhao, (2020), [arXiv:2009.06441 \[nucl-th\]](#).
- [32] E. Annala, T. Gorda, A. Kurkela, J. Nättilä, and A. Vuorinen, *Nature Phys.* (2020), 10.1038/s41567-020-0914-9, [arXiv:1903.09121 \[astro-ph.HE\]](#); *Mem. Soc. Ast. It.* **90**, 81 (2019), [arXiv:1904.01354 \[astro-ph.HE\]](#).